DOI: 10.21062/mft.2023.012 © 2023 Manufacturing Technology. All rights reserved. http://www.journalmt.com

Effect of Refined Spheroidizated Structure on Mechanical Properties of Spring Steel 51CrV4

Jakub Kotous (0000-0001-9141-8477), Daniela Nacházelová (0000-0002-0050-6859), Jaromír Dlouhý (0000-0002-1241-6121), Martin Rund (0000-0001-8655-5215)
COMTES FHT a.s., Prumyslova 995, 334 41 Dobrany. Czech Republic.
E-mail: jkotous@comtesfht.cz, dnachazelova@comtesfht.cz, jdlouhy@comtesfht.cz, mrund@comtesfht.cz.

The steel 51CrV4 is widely used for the production of springs. Materials research into spring steels aims to meet the requirements of the industry, which mainly concern high yield and tensile strengths. Ductility has to be retained as the strength is increased. Also, the resistance against brittle fracture is important, measured as fracture toughness. Enhancement of the mentioned mechanical properties can be accomplished by structural refinement. One possible way to refine the final quenched and tempered structure is to refine the soft annealed structure before quenching. The article is devoted to Accelerated Carbide Spheroidization and Refinement (ASR) with a comparison to conventional soft annealing (SA) in the 51CrV4 spring steel. Both spheroidization treatments (ASR by induction heating, and SA by electric furnace heating) led to different carbide particle sizes. The carbide refinement alters the material's behavior during quenching. Finer carbides dissolve more rapidly during austenitization at the quenching temperature. It is possible to lower the quenching temperature thanks to carbide refinement. Mechanical properties after hardening with different quenching temperatures were positively affected too.

Keywords: Accelerated Spheroidization, ASR, Refinement, Quenching, Fracture Toughness

1 Introduction

Today's trend in enterprises is to improve performance, achieve materials savings and extend the product life. To accomplish this, they may seek new and alternative materials, e.g. springs with possible weight reduction [1] or quenched spring steel with the contribution of Cu precipitation hardening [2]. But also optimize or even completely change the manufacturing technology [3–5]. The performance of spring production in an enterprise is determined by its bottlenecks. Examples of bottlenecks may include essential but time-consuming treatment steps or machines with a limited capacity. One of the long-time and often unavoidable treatment steps is soft annealing. Soft annealing is an important stage in the treatment of spring, bearing, and other types of steel [6]. Parts from spring steels are mostly subjected to alternating cyclic stresses and relaxation, which is why manufacturers strive to improve their yield strength and ultimate strength while maintaining their ductility and toughness [7–10]. Typically, high-strength spring steels are soft-annealed before hardening. In industrial practice, conventional soft annealing is ordinarily used which is very time-consuming due to slow diffusion. It may take several tens of hours [11]. Conventional soft annealing, essentially leading to carbide spheroidization, can be substituted with various methods [12–14].

The research into accelerated spheroidization of carbides in steels, i.e. ASR (Accelerated Spheroidization and Refinement) has shown that accelerated spheroidization can be initiated via heat treatment [15] or thermomechanical treatment [16]. The physical basis of the ASR involved repeated austenitizing and subsequent divorced eutectoid transformation during cooling [17, 18]. It is necessary for the divorced eutectoid transformation that some cementite remains undissolved during austenitization. Thanks to these principles, the carbide spheroidization becomes several times faster and often impacts grain refinement as well [19]. Upon subsequent quenching and tempering, the material contains uniformly dispersed finer carbides in a generally finer hardening structure. The fine structure resulting from the ASR has a favorable effect on the required quenching temperature, mechanical properties, and the life of the final parts. The yield strength and ultimate strength increase, while ductility remains unaffected. When compared to the soft-annealed condition, the material upon the ASR exhibits slightly reduced machinability. On the other hand, the fine structure after the ASR enables the required mechanical properties to be obtained using lower quenching temperatures than the soft-annealed structure. This offers significant potential for cost savings in the heat treatment of spring steels and for extending the life of parts.

2 Material and methods

The goal of the present experiment was to compare the microstructures and properties of hardened spring steel upon two annealings (carbide spheroidization) methods: conventional soft annealing (SA) and accelerated carbide spheroidization (ASR). The carbide spheroidization treatments were followed by quenching and tempering. Microstructures were examined utilizing a scanning electron microscope. The material in its various conditions was also studied using hardness testing, tensile and fracture toughness testing.

The experimental material was the 51CrV4 (according to ČSN EN 10083-1) medium-carbon chromium-vanadium spring steel whose chemical composition is given in Tab. 1 (measured with Q4 TASMAN optical emission spectrometer). It was supplied in 21 mm-diameter hot-rolled bars. The as-received microstructure consisted of bainite and a small amount of lamellar pearlite (Fig. 1). Hardness according to Vickers with a load of 10 kg was measured at 5 points for each sample. Its hardness was 345 ± 15 HV10.

Tab. 1 *Chemical composition of 51CrV4 spring steel, wt %*

C	Si	Mn	P	S	Cr	Al	V	Nb	Fe
0.51	0.27	0.96	0.015	0.017	1.07	0.003	0.138	0.002	bal.

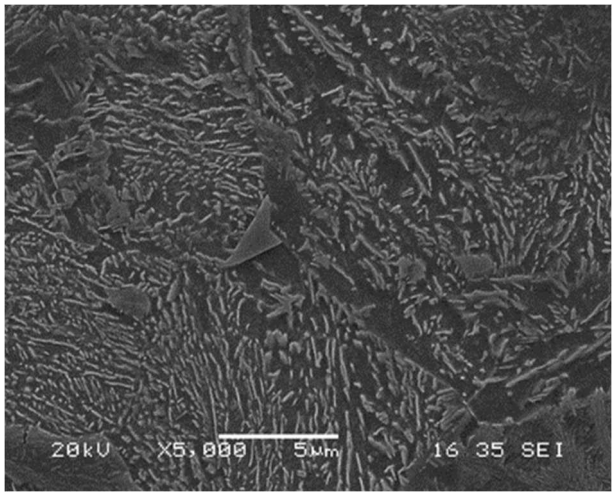

Fig. 1 *Initial microstructure of 51CrV4 spring steel, 345 HV10*

Carbide spheroidization was carried out using two different sequences and followed by quenching from various temperatures and tempering. The accelerated spheroidization process (ASR) was performed using medium-frequency (f_{max}=17 kHz) induction heating equipment with a maximum power of 25 kW. The specimens were bars 16 mm in diameter and 400 mm in length. A PLC was employed to control the heating sequence. The temperature was measured with a thermocouple welded onto the specimen. The ASR processing comprised three thermal cycles with intermediate cooling steps. In each cycle, the heating temperature was 760 °C, and the time at the temperature of 15 seconds was followed by cooling in the air. The total duration of the sequence was approximately 10 minutes.

Soft annealing (SA) was performed in an air furnace. As in the previous case, the workpieces were 16 mm-diameter bars. The thermal schedule was as follows: heating at 10 °C/ min to the temperature of 720 °C, cooling at 15 °C/ hour to 750 °C, holding for 4 hours, slow cooling at 15 °C/ hour to 720 °C, and cooling at 25 °C/ hour to 400 °C. The total time of the conventional soft annealing process was approximately 12 hours.

The spheroidization stage (ASR or SA) was followed by quenching and tempering. Heating for quenching and tempering was carried out in an air furnace. Temperatures of 800, 820, 840, and 860 °C were chosen for the experiment. The austenitizing time was 30 minutes and the material was quenched in oil. The tempering temperature and time were 450 °C and 2 hours, respectively.

After heat treatment, the specimens were examined using metallographic analysis, measurement of hardness, tensile, and fracture toughness testing. Tensile tests were carried out on tempered specimens which had been quenched from 800 and 840 °C, for both spheroidizing treatments. The test took place at an ambient temperature according to the ČSN EN ISO 6892-1 standard. For each treatment, three test pieces were tested whose dimensions are given in Fig. 2.

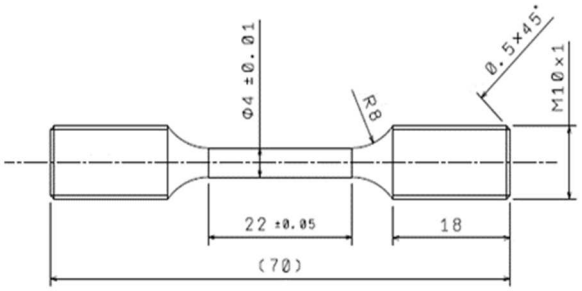

Fig. 2 *Drawing of tensile test specimen*

Two fracture toughness test specimens were made for each sequence. They were three-point bend test pieces with a notch whose shape enabled a COD extensometer to be attached (Fig. 3), for direct measurement of the notch opening.

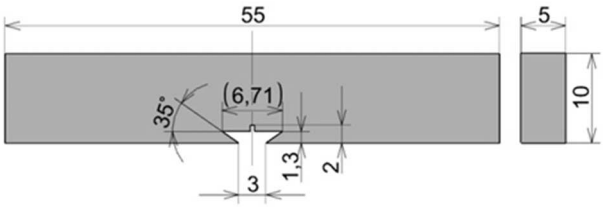

Fig. 3 *Drawing of fracture toughness test specimen*

First, a fatigue crack a_0 with a size in the desired range of 0.45–0.55 times the specimen width W was created in each specimen, having the resulting stress intensity factor of 16 MPa.m$^{0.5}$. Then, side notches were made, each with a depth of 10 % of the specimen thickness B, i.e.

$$B_N = 0.2 * B \quad (1)$$

Testing was carried out in the MTS Bionix servo-hydraulic machine at a speed of 0.5 mm/min. All specimens failed suddenly during testing without any signs of stable crack propagation. After reviewing the strength-strain plot (example in

Fig. 10), the ASTM E1921 international standard was chosen, which relies on the elastic-plastic approach for evaluating fracture toughness K_{Jc}.

3 Results

3.1 Carbide spheroidization

The microstructures obtained by the ASR (Fig. 4) and soft annealing (Fig. 5) consist of a ferritic matrix and spheroidized carbides. The main differences between them lie in the sizes and densities of carbide particles. The size of the spheroidized carbides after the ASR is between 100 and 300 nm (Fig. 4). After conventional soft annealing, the size of the spheroidized carbides is between 500 and 1000 nm (Fig. 5). Hardness after the ASR reached 232 HV10, whereas the hardness value after soft annealing was 179 HV10. The difference is due to the different sizes and densities of carbides. After the ASR, the carbides are finer and their density in the matrix is higher. As a result, they provide greater strengthening.

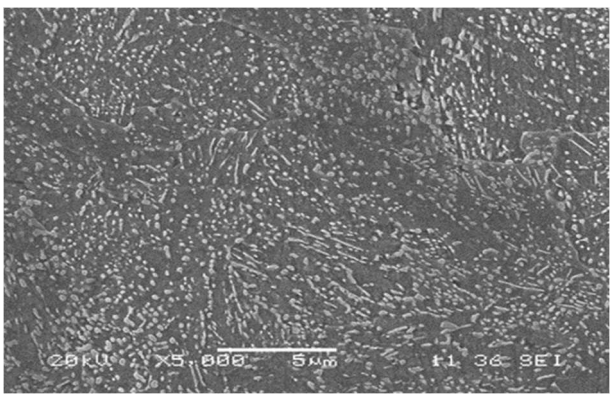

Fig. 4 *Microstructure after accelerated spheroidization (ASR), 232 HV10*

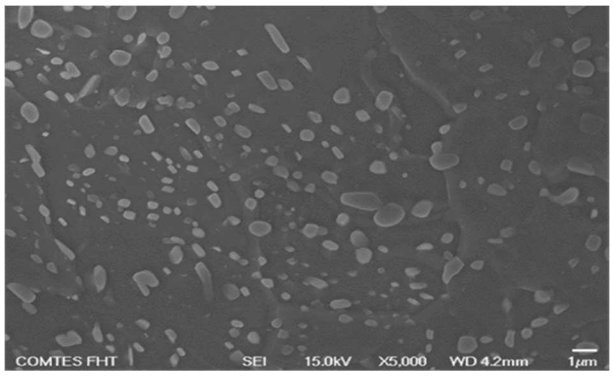

Fig. 5 *Microstructure after soft annealing (SA), 179 HV10*

3.2 Hardening

The as-quenched microstructures consist of martensite and undissolved carbides. After quenching from 800 °C, the microstructures obtained by both processes contain numerous undissolved carbides. The microstructure upon the ASR and hardening contains finer martensite plates and finer undissolved carbides (Fig. 6) when compared to the microstructure obtained by hardening after soft annealing (Fig. 7). After both ASR and soft annealing, the carbides are mostly found within prior austenite grains. Likely, their density and size are not sufficient to pin the austenite grain boundaries and prevent grain growth. Prior austenite grain sizes are substantially equal after the ASR and after soft annealing. It was about 4.5 µm.

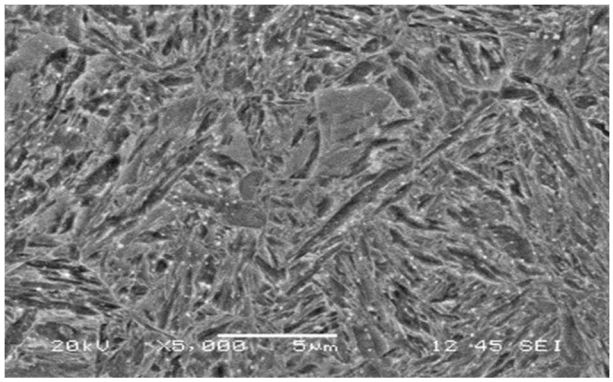

Fig. 6 *Microstructure of the sample ASR/800 Q (ASR, quenching from 800 °C), 677 HV10*

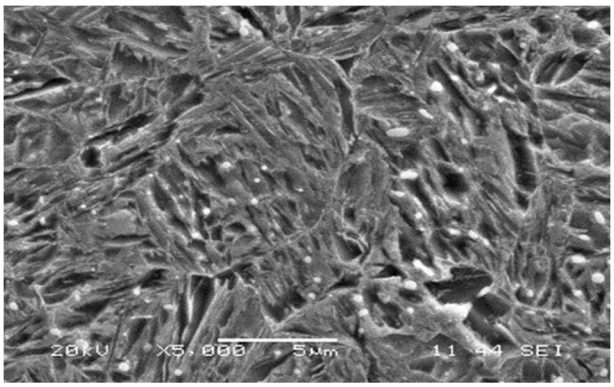

Fig. 7 *Microstructure of the sample SA/800 Q (soft annealing, quenching from 800 °C), 624 HV10*

Final microstructures after quenching and tempering consist of tempered martensite and undissolved spheroidized carbides. Tempering caused cementite to precipitate within the martensitic matrix but no differences between the sizes, shapes, or distribution of these particles were found between the specimens upon the ASR and soft annealing.

As the quenching temperature was raised to 860 °C in the subsequent sequences, the number of undissolved carbides diminished. In the ASR sequence, most carbides became dissolved at the quenching temperature as low as 820 °C. Upon the highest quenching temperature, 860 °C, undissolved carbides were only rarely found (Fig. 8). After soft annealing and hardening, the ferritic matrix still contains a large amount of undissolved carbides (Fig. 9). Martensite obtained by hardening upon the ASR does not appear finer when compared to martensite obtained upon soft annealing.

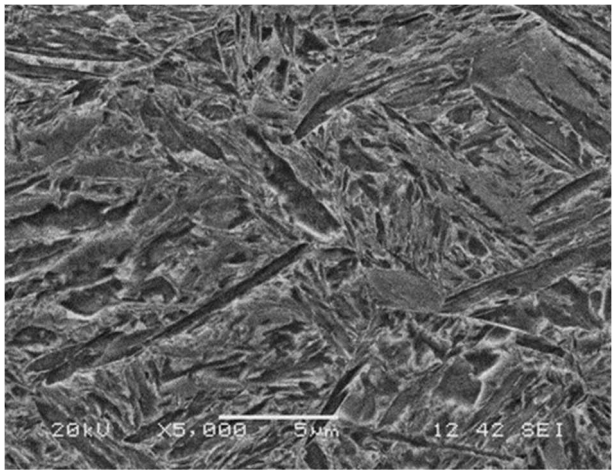

Fig. 8 *Microstructure of the sample ASR/860 Q (ASR, quenching from 860 °C), 706 HV10*

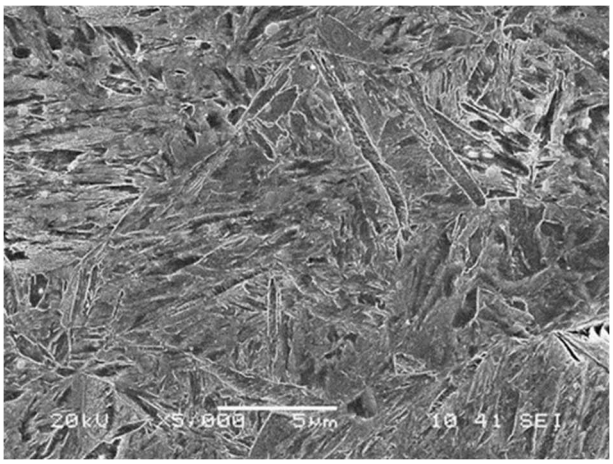

Fig. 9 *Microstructure of the sample SA/860 Q (SA, quenching from 860 °C), 679 HV10*

3.3 Hardness

Hardness according to Vickers (ČSN EN ISO 6507-1) with a load of 10 kg was measured at 5 points for each sample. Hardness levels after quenching and tempering are shown in Tab. 2. The ASR process led to higher hardness upon quenching and tempering when compared to soft annealing. After soft annealing, the resulting hardness tends to increase with the quenching temperature. This is due to a more complete dissolution of carbides during austenitization. With the ASR, this was only found to occur between the quenching temperatures of 800 and 820 °C. At higher temperatures, the hardness levels were similar. The same hardness was obtained after quenching from 800 °C following the ASR and after quenching from 860 °C following soft annealing. This means that in this steel, 51CrV4, the ASR can reduce the required quenching temperature by 60 °C while providing the same final hardness.

Tab. 2 *Hardness HV10 after quenching and tempering*

Quenching temperature [°C]	ASR		Soft annealing (SA)	
	Quenching	Tempering	Quenching	Tempering
800	677 ± 4	433 ± 7	624 ± 2	406 ± 5
820	705 ± 7	443 ± 8	650 ± 2	419 ± 3
840	692 ± 7	446 ± 9	660 ± 9	424 ± 5
860	706 ± 9	447 ± 2	679 ± 7	434 ± 8

3.4 Tensile test

The tensile test results (Tab. 3) are in agreement with the measured hardness levels. Upon the ASR, the material exhibits higher yield strength and ultimate strength than upon soft annealing. The increase in the quenching temperature from 800 to 840 °C led to higher strengths in both cases.

Tab. 3 *Tensile test data*

Spheroidization	Quenching temp. [°C]	YS [MPa]	UTS [MPa]	EL [%]	R [%]
ASR	800	1402 ± 11	1465 ± 12	9.3 ± 0.8	40.9 ± 5.0
	840	1424 ± 15	1504 ± 14	9.7 ± 0.5	43.4 ± 2.0
Soft annealing (SA)	800	1298 ± 11	1360 ± 6	10.9 ± 0.2	43.9 ± 0.7
	840	1356 ± 9	1425 ± 10	10.8 ± 0.6	46.1 ± 1.5

Where:
YS…Yield strength [MPa],
UTS…Ultimate strength [MPa],
EL…Total plastic elongation [%],
R…Reduction of area [%].

3.5 Fracture toughness

The sequences chosen for fracture toughness testing were the same as those for tensile testing (ASR/SA, quenching temperatures 800 and 840 °C, tempering). The strength-strain plots (example in Fig. 10) were achieved and evaluated fracture toughness K_{Jc}.

An example of a fracture surface is given in Fig. 11, where one can distinguish the initial fatigue crack a_0 and the brittle (unstable) crack propagation region indicating the final separation. In all specimens, the final separation surfaces exhibited identical dimples (Fig. 11). Fracture toughness K_{Jc} corresponding to unstable crack propagation was evaluated. The results of this test are listed in Tab. 4.

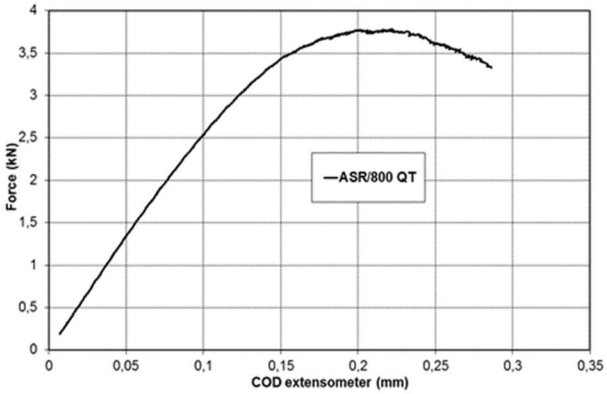

Fig. 10 *Example of the stress response plot for the specimen ASR 800 QT*

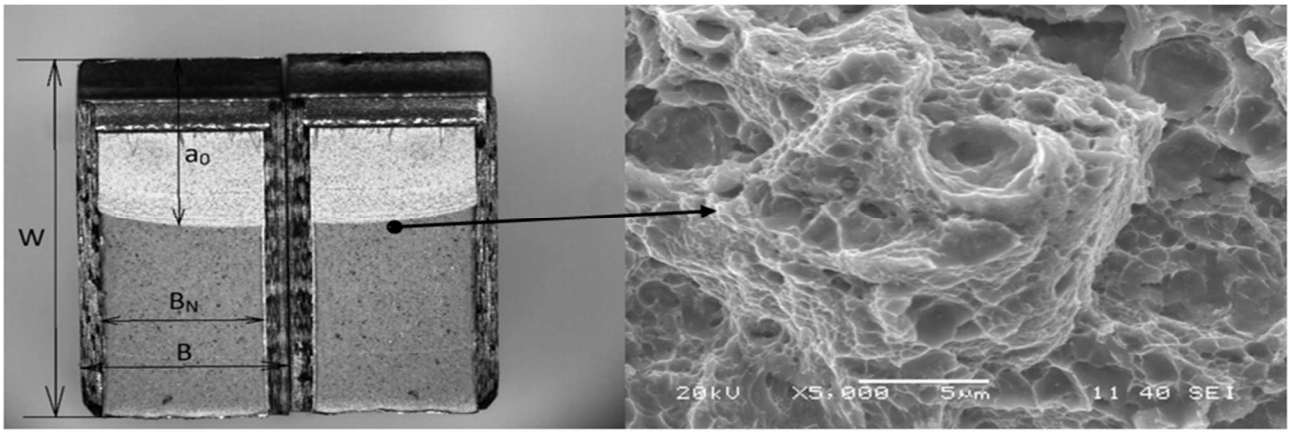

Fig. 11 *Fracture surface with dimple morphology of the specimen SA 840 QT_2*

Tab. 4 *Initial dimensions and results of the fracture toughness*

Spheroidization	Q_t [°C]	W [mm]	B [mm]	B_N [mm]	a_0 [mm]	J_c [kN/m]	K_{Jc} [MPa*m$^{1/2}$]
ASR	800	10.03	4.97	3.91	5.68	79.4	137.7
		10.03	4.99	3.86	4.97	84.4	142.0
	840	10.03	4.93	3.93	4.25	58.9	118.6
		10.03	5.01	3.89	4.54	44.0	102.5
Soft annealing (SA)	800	10.03	5.01	3.88	4.26	83.7	141.3
		10.03	5.01	3.87	5.65	71.4	130.6
	840	10.03	4.98	3.88	4.58	82.7	140.5
		10.06	4.98	3.88	5.17	74.0	132.9

Where:
Qt…Quenching temperature [°C],
W…Specimen width [mm],
B…Specimen thickness [mm],
B_N…Specimen net thickness [mm],
a_o…Crack length [mm],
J_c…Elastic plastic J-integral at the onset of cleavage fracture [kN/m],
K_{Jc}…Fracture toughness expressed in terms of an elastic-plastic stress intensity factor, K_{Jc}, that is derived from the J-integral calculated at fracture.

The results show that increasing the quenching temperatures had a significant effect on the decrease in fracture toughness values upon the ASR, whereas, in the material upon SA, no effect of the increase in quenching temperatures was found.

4 Discussion

The quenching temperature determines the degree of dissolution of carbides, and thereby the concentration of carbon in austenite. Undissolved carbides may act as obstacles that prevent austenite grain growth during austenitizing, and the growth of martensite crystals during subsequent quenching. In the soft-annealed material, a gradual loss of undissolved carbides with increasing quenching temperature was observed. Corresponding to this is the trend of growing hardness after both quenching and tempering. Yield strength and ultimate strength, too, differ greatly between the quenching temperatures of 800 and 840 °C.

A different trend was found in the material upon the ASR, as described below. All carbides had dissolved during austenitizing at a temperature as low as 820 °C. Further increases in the quenching temperature had no potential for substantially increasing the carbon content in austenite. Mechanical properties are in agreement with this finding. Upon quenching from the temperature of 820 °C and above, the hardness levels are practically equal. The difference between the yield strength and the ultimate strength between the quenching temperatures of 800 °C and 840 °C is smaller here than in the material upon SA. Microstructure observation showed that upon quenching from 800 °C, the martensitic matrix in the ASR specimens was finer than in the SA ones, whereas, upon 860 °C, there was no perceptible difference between the sizes of martensite crystals.

After quenching from 800 °C, the fracture toughness values of the ASR and the SA materials were identical. Upon quenching from 840 °C, the fracture toughness of the ASR material decreased. This corresponds to the dissolution of virtually all carbides and the coarsening of martensite, as confirmed by metallographic observation. Fracture toughness tests revealed that the optimum quenching temperature of the ASR material was lower than that of the SA material. Upon quenching from 840 °C, the strength values of the ASR material were high and its ductility did not decrease, although the decrease in fracture toughness reflected the coarsening of the structure.

5 Conclusion

The 51CrV4 spring steel was heat treated to refine its microstructure and improve its mechanical properties. A comparison was made between the structures and properties of quenched and tempered specimens after the accelerated annealing process ASR and after conventional soft annealing. The ASR produced finer carbides and finer subsequent martensitic structure upon hardening that is to say at the quenching temperature of 800 °C. Upon the ASR and quenching from 840 °C, martensite plates became equally coarse as those in the conventionally soft-annealed material. The strength characteristics of the quenched and tempered material were higher upon the ASR than upon conventional soft annealing, regardless of the quenching temperature. The fracture toughness of the ASR material that was quenched from 800 °C was similar to that of the soft-annealed and heat-treated material. After the quenching temperature had been raised to 840 °C, the ASR material showed a decrease in fracture toughness due to the dissolution of all carbides in the structure and martensite coarsening. The experiments have shown that the ASR process enables the quenching temperature to be reduced by 40–60 °C, improves strength characteristics, and maintains ductility and fracture toughness levels in the material.

Acknowledgement

The result was supported from ERDF Research of advanced steels with unique properties, No. CZ02.1.01/0.0/0.0/16_019/0000836.

References

[1] HÁJEK, J., NOVÝ, Z., KUČEROVÁ, L., JIRKOVÁ, H., SALVETR, P., MOTYČKA, P., HAJŠMAN, J. and BYSTŘICKÁ, T. (2022). A New Alloying Concept for Low-Density Steels. In: *Materials*, Vol. 15, pp. 2539

[2] SALVETR, P., NOVÝ, Z., GOKHMAN, A., KOTOUS, J., ZMEKO, J., MOTYČKA, P. and DLOUHÝ, J. (2020). Influence of Si and Cu Content on Tempering and Properties of 54SiCr6 Steel. In: *Manufacturing Technology*, Vol. 20, No. 4, pp. 516–520, ISSN 12132489

[3] FRAGOUDAKIS, R., KARDITSAS, S., SAVAIDIS, G. and MICHAILIDIS, N. (2014).

The effect of heat and surface treatment on the fatigue behaviour of 56SiCr7 spring steel. In: *Procedia Engineering*, Vol. 74, pp. 309–312, ISSN 18777058

[4] PRABHAKARAN, S. and KALAINATHAN, S. (2016). Compound technology of manufacturing and multiple laser peening on microstructure and fatigue life of dual-phase spring steel. In: *Materials Science and Engineering A*, Vol. 674, pp. 634–645, ISSN 09215093

[5] JANDA, T., JIRKOVÁ, H., JENÌČEK, Š. and KUČEROVÁ, L. (2019). Influence of cooling rate on microstructure and mechanical properties of 42SiCr steel after Q&P process. In: *Manufacturing Technology*, Vol. 19, No. 4, pp. 583–588, ISSN 12132489

[6] SONG, W., CHOI, P.-P., INDEN, G., PRAHL, U., RAABE, D. and BLECK, W. (2014). On the spheroidized carbide dissolution and elemental partitioning in a high carbon bearing steel 100Cr6. In: *Metallurgical and Materials Transactions A*, Vol. 45, pp. 595–606

[7] GARIBOLDI, E., NICODEMI, W., SILVA, G., VEDANI, M. (1994). Effect of tempering level on mechanical properties and toughness of spring steels. In: *Materials Science Forum*, Vol. 163, No. 6, pp. 107–114, ISSN 02555476

[8] GIANNAKIS, E., MALIKOUTSAKIS, M. and SAVAIDIS, G. (2016). Fatigue Design of Leaf Springs for New Generation Trucks. In: *IOP Conference Series: Materials Science and Engineering*, Vol. 161, pp. 1-10, ISSN 1757899X

[9] PYTTEL, B., BRUNNER, I., KAISER, B., BERGER, C. and MAHENDRAN, M. (2014). Fatigue behaviour of helical compression springs at a very high number of cycles - Investigation of various influences. In: *International Journal of Fatigue*, Vol. 60, pp. 101–109, ISSN 01421123

[10] JANDA, T. (2018). Use of metallographic analysis for evaluating microstructures in quenched and tempered high-strength steel. In: *Manufacturing Technology*, Vol. 18, No. 1, pp. 47–52, ISSN 12132489

[11] NAM, W.J., BAE, C.M. (1999). Coarsening behavior of cementite particles at a subcritical temperature in a medium carbon steel. In: *Scripta Materialia*, Vol. 4, No. 3, pp. 313–318

[12] KUČEROVÁ, L., JIRKOVÁ, H., MAŠEK, B. (2015). Various approaches to accelerated Carbide spheroidization of 54SiCr steel. In: *Key Engineering Materials*, Vol. 647, pp. 3–8, ISBN 9783038354703

[13] HARISHA, S.R., SHARMA, S., KINI, U.A. and GOWRI SHANKAR, M.C. (2018). Study on Spheroidization and Related Heat Treatments of Medium Carbon Alloy Steels. In: *MATEC Web of Conferences*, Vol. 144, pp. 1–10, ISSN 2261236X

[14] SAHA, A., MONDAL, D.K. and MAITY, J. (2011). An alternate approach to accelerated spheroidization in steel by cyclic annealing. In: *Journal of Materials Engineering and Performance*, Vol. 20, pp. 114–119, ISSN 10599495

[15] HAUSEROVA, D., DLOUHY, J., NOVÝ, Z. (2014). Effect of heating rate on accelerated carbide spheroidisation (ASR) in 100CrMnSi6-4 bearing steel. In: *Archives of Metallurgy and Materials*, Vol. 59, No. 3, pp. 1199–1203, ISSN 17333490

[16] HAUSEROVA, D., DLOUHY, J., NOVY, Z. (2014). Accelerated carbide spheroidisation and refinement (ASR) of the C45 steel during controlled rolling. In: *Materiali in Tehnologije*, Vol. 48, No. 5, pp. 797–800, ISSN 15803414

[17] TIAN, Y.L., KRAFT, R.W. (1987). Mechanisms of Pearlite Spheroidization. In: *Metallurgical Transactions*, Vol. 18A, pp. 1403–1414

[18] MAITY, J., SAHA, A., MONDAL, D.K. and BISWAS, K. (2013). Mechanism of accelerated spheroidization of steel during cyclic heat treatment around the upper critical temperature. In: *Philosophical Magazine Letters*, Vol. 93, No.4, pp. 231–237, ISSN 09500839

[19] DLOUHY, J., HAUSEROVA, D., NOVY, Z. (2016). Influence of the carbide-particle spheroidisation process on the microstructure after the quenching and annealing of 100CrMnSi6-4 bearing steel. In: *Materiali in Tehnologije*, Vol. 50, No. 1, pp. 159–162, ISSN 15803414